



Published in final edited form as:

ACS Chem Biol. 2013 October 18; 8(10): 2322–2330. doi:10.1021/cb400541z.

## Complexity generation in fungal polyketide biosynthesis: a spirocycle-forming P450 in the concise pathway to the antifungal drug griseofulvin

Ralph A. Cacho<sup>1</sup>, Yit-Heng Chooi<sup>1,3</sup>, Hui Zhou<sup>1,4</sup>, and Yi Tang<sup>1,2,\*</sup>

<sup>1</sup> Department of Chemical and Biomolecular Engineering, University of California, Los Angeles, 420 Westwood Plaza, Los Angeles, CA 90095

<sup>2</sup> Department of Chemistry and Biochemistry, University of California, Los Angeles, 607 Charles E. Young Drive East, Los Angeles, CA 90095

### Abstract

Griseofulvin (**1**) is a spirocyclic fungal natural product used in treatment of fungal dermatophytes. Formation of the spirocycle, or the grisan scaffold, from a benzophenone precursor is critical for the activity of **1**. In this study, we have systematically characterized each of the biosynthetic enzymes related to the biogenesis of **1**, including the characterization of a new polyketide synthase GsfA that synthesizes the benzophenone precursor and a cytochrome P450 GsfF that performs oxidative coupling between the orcinol and the phloroglucinol rings to yield the grisan structure. Notably, the finding of GsfF is in sharp contrast to the copper-dependent dihydrogeodin oxidase that performs a similar reaction in the geodin biosynthetic pathway. The biosynthetic knowledge enabled the *in vitro* total biosynthesis of **1** from malonyl-CoA using all purified enzyme components. This work therefore completely maps out the previously unresolved enzymology of the biosynthesis of a therapeutically relevant natural product

### Keywords

Antifungal; polyketides; cytochrome P450

Griseofulvin (**1**), a polyketide produced by ascomycetes such as *Penicillium aethiopicum*,<sup>1</sup> is the first oral antifungal drug<sup>2-4</sup> and has been in use for many years in medical and veterinary applications.<sup>5</sup> While **1** is largely superseded by newer antifungal drugs such as azoles and echinocandins, **1** has a niche in treatment of dermatophytes such as *tinea capitis* (ringworm

\* Corresponding Author yitang@ucla.edu.

<sup>3</sup> Present Address: Research School of Biology, Australian National University, Acton ACT 0200, Australia

<sup>4</sup> Present address: Department of Biological Engineering, Massachusetts Institute of Technology, Synthetic Biology Center, 500 Technology Square, Cambridge, MA 02139

#### ASSOCIATED CONTENT

**Supporting Information.** Supplemental material and methods. NMR spectrum tables. This material is available free of charge via the Internet at <http://pubs.acs.org>.

#### Author Contributions

The manuscript was written through contributions of all authors. All authors have given approval to the final version of the manuscript.

of the scalp) and *tinea pedis* (athlete's foot). **1** recently gained medical attention due to its ability to disrupt mitotic spindle<sup>6</sup> and act as potential inhibitor of centrosomal clustering<sup>7</sup> in tumor cells. From a biosynthetic perspective, **1** occupies a place in the pantheon of natural products due to its significance in establishing the field of study of polyketide biosynthesis.<sup>8</sup> The acetate origin of the carbon skeleton of **1** was demonstrated through the feeding of [1-<sup>14</sup>C]-acetate to the griseofulvin-producing strain *Penicillium griseofulvum* Dierckx and the labeling pattern in **1** was determined using degradation experiments.<sup>9, 10</sup> The polyketide hypothesis<sup>11</sup> was further confirmed through feeding of singly and doubly [<sup>13</sup>C]-acetate followed by NMR analysis (Figure 1).<sup>12</sup> In addition, the formation of the spirocyclic grisan ring of **1** was an examples used to illustrate the prevalence of phenol oxidative coupling reactions in Nature.<sup>13</sup> Subsequent studies using feeding of the radiolabeled benzophenone intermediates griseopheone B (**10**) and C (**11**) implicated their role in the biosynthesis of **1** and supported further suggests the requirement of oxidative coupling to form the grisan ring.<sup>14-16</sup>

Despite these pioneering studies, the genetic and biochemical basis of the biosynthetic pathways of **1** have been left unexplored. Considering the importance of **1** to the field of natural products, specifically the polyketide community, the complete understanding of how its carbon backbone is assembled and is subsequently transformed into **1** is therefore compelling. We recently sequenced the genome of *P. aethiopicum* to map its biosynthetic capacity.<sup>17</sup> In addition to **1** and the related metabolite dechlorogriseofulvin (**2**), *P. aethiopicum* also produces viridicatumtoxin (**3**) and tryptoquialanine (**4**), two other secondary metabolites with spirocyclic moiety (Figure 1B).<sup>1, 17, 18</sup> Bioinformatic mining of the *P. aethiopicum* genome led to the discovery of the putative *gsf* cluster (Figure 1C), which contains *gsfA*, a gene for a non-reducing polyketide (NR-PKS) and genes for tailoring enzymes that appear consistent with the modifications required to form **1**. Gene deletion of *gsfA* and flavin-dependent halogenase gene *gsfI* confirmed the association between *gsf* cluster and biosynthesis of **1**.<sup>17</sup> The enzymology of the NR-PKS, which synthesizes a polyketide backbone atypical to the characterized aromatic polyketides, and the enzymes involved in maturation of the griseofulvin scaffold structure, highlighted by the spirocyclic grisan ring, can now be studied using modern genetic and biochemical tools. In this work, we present the comprehensive single-gene knockout and *in vitro* reconstitution of every enzyme in the *gsf* pathway. These insights led to the *in vitro* synthesis of **1** from malonyl-CoA using purified *gsf* enzymes and cofactors.

## RESULTS AND DISCUSSION

### GsfA is a norlichexanthone synthase

Our initial genetic studies with *P. aethiopicum* showed that *gsfA*, which encodes a thioesterase (TE)-less NR-PKS, is required to produce the heptaketide backbone of **1**.<sup>17</sup> To biochemically investigate the role of GsfA, *gsfA* cDNA was cloned into the YEplac195 yeast-*E. coli* shuttle vector driven by the ADH2 promoter. The resulting YepLac195-GsfA construct was transformed into *S. cerevisiae* BJ5464-NpgA strain, which contain a chromosomal copy of *npgA*, the phosphopantetheine transferase gene from *Aspergillus nidulans* which post- translationally installs the phosphopantetheine arm to the acyl carrier

protein (ACP) domain of PKS.<sup>19</sup> Intact holo-GsfA (185 kDa) with a C-terminal His-tag was purified to near homogeneity to a final titer of 2 mg/L of yeast culture.

To assay the activity of recombinant GsfA, we incubated the enzyme with either malonyl-CoA directly or with an *in situ* malonyl-CoA generation system (Figure 2). Furthermore, since GsfA lacks a TE domain that may release the mature polyketide product and no standalone TE is found in the gene cluster, we incubated GsfA with a promiscuous TE domain from the hypothemycin NR-PKS Hpm3.<sup>20</sup> Surprisingly, GsfA alone was sufficient for the production and release of a predominant product **5** with  $m/z=259$ ,  $[M+H]^+$  (Figure 2). Addition of the Hpm3 TE domain did not enhance the turnover of the product **5**. To purify sufficient amount of **5** for structural characterization, we cultured the BJ5464-NpgA strain expressing GsfA, which was able to produce **5** at a final titer of 10 mg/L. Compound purification followed by NMR characterization identified **5** as norlichexanthone (Figure 2), which bears the expected heptaketide backbone.

A typical NR-PKS contains starter-unit-ACP transacylase (SAT),<sup>21</sup> ketosynthase (KS), malonyl-CoA-ACP transacylase (AT), product template (PT),<sup>22, 23</sup> ACP and TE domains.<sup>24-28</sup> The cyclization regioselectivity of the nascent polyketide chain is determined by the functions of the PT and the TE domains.<sup>22-24</sup> The PT domain, in particular, mediates the regioselective aldol-type cyclization through steric interactions with the newly-formed polyketide.<sup>22, 23</sup> Using phylogenetic analysis and domain shuffling experiment, we previously classified ~100 PT domains into distinct clades based on ring size and first aldol condensation regioselectivity.<sup>29</sup> Interestingly, the GsfA PT does not classify into any of the clades, in correspondence with its unique cyclization selectivity. Indeed, based on previous labeling studies and the biochemical studies using purified GsfA, we can conclude that GsfA PT must catalyze the unusual C8-C13 aldol condensation as the first cyclization step in the formation of **5**.

The enzymatic basis of the Claisen-like condensation (C1-C6) to afford the phloroglucinol ring, however, is unclear. GsfA belongs to a TE-less NR-PKS, of which no terminal TE domain is found in the NR-PKS. For TE-less NR-PKSs, a standalone  $\beta$ -lactamase-like enzyme is typically present in the gene cluster to release the product either through hydrolysis or Claisen-like condensation.<sup>30</sup> No gene for such releasing enzyme is present in the *gsf* cluster, and our reconstitution studies show that GsfA alone is able to turnover products. Therefore the activities to catalyze the C1-C6 cyclization must be within the GsfA NR-PKS. It is reasonable to propose that because of the smaller size of the polyketide, the PT domain, when distorting the polyketide backbone for the aldol cyclization, may also promote the C1-C6 cyclization in its active site. Hence, formation of **5** represents an intriguing example in which a NR-PKS performs a Claisen-like cyclization without using a dedicated, in-line or dissociated TE. While the two cyclization events in the biosynthesis of **5** (and **5a**) are unusual, it is far from unique. To wit, compounds bearing the norlichexanthone scaffold have been isolated from lichens.<sup>31</sup> Thus one can reasonably speculate that a GsfA homolog may be found in the fungal symbionts in the lichens that produce compounds related to **5**.

## Methylation of GsfA product by GsfB and GsfC hinders xanthone formation

Although the xanthone **5** is detected as the only polyketide product from the *in vitro* assay, it is most likely that the true heptaketide product of GsfA is the benzophenone **5a** (Table 1), which can undergo a spontaneous dehydration to form **5**. Formation of the grisan structure in **1** must proceed through the intermediate **5a**, thereby making **5** a likely off-pathway shunt product. Indeed, feeding of **5** to the *gsfA* mutant did not restore the production of **1** (Figure S1), thereby ruling out the possibility of **5** undergoing rehydration to open the xanthone ring and form **5a** during biosynthesis of **1**. We hypothesize that the methylation of the phenols in **5a**, especially at 9-OH may hinder dehydration and suppress xanthone formation. To investigate this hypothesis, genetic inactivation and *in vitro* reconstitution of the three *O*-methyltransferases (MTs) GsfB, GsfC and GsfD were performed. Deletion of *gsfB* led to the production of **5** as a minor product, **7** (obs.  $m/z = 291$ ,  $[M+H]^+$ ), **8** (obs  $m/z = 325$ ,  $[M+H]^+$ ), and **9** (obs.  $m/z = 337$ ,  $[M+H]^+$ ) (Figure 3, ii). Elucidation of the structures of the compounds using 1D  $^1H$  and  $^{13}C$  and 2D HSQC and HMBC NMR revealed the identity of **7** as griseophenone E, **8** as griseophenone F and **9** as desmethyl-dehydrogriseofulvin B. **7-9** share the characteristic lack of methylation at 3-OH, suggesting that GsfB is the 3-OH MT. The isolation of **9** also suggests that downstream steps, including the formation of the grisan structure, are not dependent on the 3-OH methylation step. On the other hand, the *gsfC* mutant showed **5** as a more prominent product in comparison to the metabolic profile of the *gsfB*, along with **6** (obs.  $m/z = 291$ ,  $[M+H]^+$ ), **16** (obs.  $m/z = 273$ ,  $[M+H]^+$ ) and **17** (obs.  $m/z = 325$ ,  $[M+H]^+$ ), which were identified as griseophenone D, griseoxanthone C and griseophenone H respectively (Figure 3, iv). In contrast to the metabolites found in *gsfB* mutant, **6**, **16** and **17** are methylated at 3-OH, but lack methylation at 9-OH, thereby confirming that GsfC is the 9-OH MT. Isolation of these benzophenone intermediates in the *gsfB* and *gsfC* mutants confirms our hypothesis that methylations at 3-OH and more so at 9-OH, can suppress the formation of the off-pathway shunt product **5**.

In order to verify the roles of the MTs, *in vitro* assay of GsfA together with each of the recombinant MT was performed. The coupled reaction with GsfA generates the labile benzophenone **5a** *in situ* that serve as substrates for the MTs. Assay containing GsfA and GsfB produced predominantly xanthenes **5** and **16**, as well as **6**, demonstrating partial suppression of dehydration after methylation of 3-OH (Figure 3, v). Presumably, **6** undergoes dehydration to form **16**. Alternatively, the nascent polyketide product of GsfA undergoes dehydration to **5** followed by methylation by GsfB to form **16**. The coupled assay of GsfA with GsfC, on the other hand, produced predominantly **7** as expected, with a trace amount of **5**, further confirming the 9-OH methylation step as a means to keep the GsfA product **5a** on pathway during biosynthesis of **1** (Figure 3, iii). Taken together, these studies with MTs confirm that the GsfA product undergoes methylation by both GsfB and GsfC before forming the grisan ring, which is in agreement of the previous feeding studies.<sup>14, 15</sup>

On the other hand, knockout of *gsfD* yielded the production of grisan-containing compounds desmethyl-dechlorogriseofulvin (**13**) (obs.  $m/z = 305$ ,  $[M+H]^+$ ), desmethyl-dehydrogriseofulvin A (**14**) (obs.  $m/z = 337$ ,  $[M+H]^+$ ), and desmethyl-griseofulvin (**15**) (obs.  $m/z = 339$ ,  $[M+H]^+$ ) (Figure 4, iii). These metabolites represent late-stage shunt products (**13** and **15**) and intermediate (**14**) during the formation of **1**. The structures of **13-15** show the

lack of methylation at the 5-OH position, implying that GsfD regioselectively targets 5-OH. Based on these results, we propose the role of GsfD is to methylate of **14** to produce dehydrogriseofulvin (**18**).

### Biochemical confirmation of the role of GsfI

Previously, loss of **1** and sole production of **2** were observed when the gene *gsfI* encoding the flavin-dependent halogenase was deleted in *P. aethiopicum*.<sup>17</sup> To biochemically reconstitute the halogenation reaction, we cloned, expressed and purified GsfI and performed an *in vitro* assay using **10**, the proposed intermediate from the previous labeling studies,<sup>15</sup> as substrate. In order to regenerate the reduced flavin cofactor of GsfI, the NADPH-dependent flavin reductase SsuE was added to the reaction. As expected, assay of the non-chlorinated **10** with GsfI led to the production of chlorinated phenone **11** at ~50% conversion (Figure S4), reflecting the ratio of the chlorinated final compound **1** and its dechlorinated counterpart **2** in the original host.

### GsfF performs phenolic coupling to afford the grisan scaffold

Oxidation of the phenone ring to form the grisan ring dramatically transforms the phenone scaffold of griseophenone B (**11**) into the spirocyclic grisan compound **14**, thereby dearomatizing the orcinol ring of **11** and creating the cyclohexadienone in **14**. An analogous reaction during biosynthesis of geodin in *A. terreus* was proposed to be catalyzed by copper-centered enzyme dehydrogeodin oxidase.<sup>32</sup> However, such a copper laccase enzyme is not encoded in the *gsf* cluster, thus we proposed that the cytochrome P450 (CYP) GsfF may instead catalyze the phenolic coupling reaction of **11** to afford **14**.<sup>17</sup> To probe the role of GsfF, we deleted *gsfF* in *P. aethiopicum* and characterized the resulting metabolites via LC-MS and NMR. The *gsfF* strain produced griseophenone C (**10**) (obs.  $m/z = 305$ ,  $[M+H]^+$ ), monochlorinated **11** (obs.  $m/z = 339$ ,  $[M+H]^+$ ) and dichlorinated griseophenone G (**12**) (obs.  $m/z = 373$ ,  $[M+H]^+$ ) (Figure 4, ii). Accumulation of **10** and **11** as major intermediates supports the coupling role of GsfF in the pathway. The degrees of chlorination of the metabolites were further ascertained based on the presence of the expected 3:1 isotopic distribution of the monochlorinated **11** and the 1.5:1 isotopic distribution of the dichlorinated **12** (Supporting Information). The C2-regioselectivity of the first chlorination reaction was determined by the loss of the symmetry along the C3-C6 axis of **11** in comparison to **10**, as evident in comparative NMR analysis. The symmetry along C3-C6 axis as shown in the NMR spectra was restored upon further chlorination of **11** to afford **12**, thus confirming the regioselectivity of the second chlorination at C4.

To functionally confirm the role of GsfF, the CYP was expressed in *S. cerevisiae* BJ5464-NpgA strain together with the *A. terreus* CYP oxidoreductase (CPR) using Gal1 and Gal10 bidirectional promoter,<sup>33</sup> allowing the temporal coexpression of the CYP and the CPR that is required for turnover of the CYP. Following induction of GsfF and CPR expression, **11** was supplemented to the yeast culture at a final concentration of 1  $\mu$ M. The organic metabolites were extracted twenty-four hours later with ethyl acetate and analyzed by LCMS. *S. cerevisiae* cells expressing both CPR and GsfF were able to completely convert **11** to a product that is identical (UV, mass and retention time) to **14** isolated from *gsfD* mutant (Figure 5, ii). In contrast, yeast cells expressing only CPR did not show any

conversion of **11** (Figure 5, i). To further prove the conversion of **11** to **14** is catalyzed by GsfF, microsomal fraction from yeast cells coexpressing CPR and GsfF was isolated and *in vitro* assay was performed in the presence of NADPH. Microsomes containing both GsfF and CPR facilitated 90% conversion of **11** to **14** after overnight incubation (Figure 5, iv). Time course kinetics of GsfF revealed conversion of **11** to **14** at a turnover rate of  $0.437 \mu\text{M min}^{-1}\cdot\text{mg}^{-1}$  of microsomal protein (Supporting Information). In contrast, identically prepared microsomes containing only CPR did not show any conversion (Figure 5, iii). Therefore, we unequivocally confirmed the role of GsfF in the oxidative formation of the spirocyclic grisan.

In this coupling reaction, the orcinol ring is contorted leading to the metamorphosis of the di-aromatic **11** into the tricyclic **14**. Based on the feeding studies in the biosynthesis of **1** using [1,1- $^{18}\text{O}$ ]-labeled acetate, all of the oxygen atoms in **1** originated from acetate.<sup>34</sup> Based on known reactions catalyzed by cytochrome P450, one can propose two different mechanisms for GsfF reaction (Scheme 2): A.) a di-radical mechanism and B.) a mechanism involving the formation of an arene oxide intermediate (**11b**). In the first mechanism, the reaction is initiated by the formation of Compound I, the active form of the heme cofactor of GsfF. Compound I then abstracts a hydrogen atom from **11** to form the resonance-stabilized phenoxy radical on the orcinol ring. Thereafter, Compound II form of GsfF abstracts the second hydrogen atom from **11a** to form the phenoxy radical on the phloroglucinol ring with water as the by-product of the reaction. The incipient phloroglucinol radical then couples with the orcinol radical in a stereospecific fashion to form **14**. This di-radical mechanism, first envisioned by Barton and Cohen,<sup>13</sup> has also been proposed for the mechanisms of the coupling between the isoquinoline and phenolic rings in reticuline by salutaridine synthase during morphine biosynthesis,<sup>35</sup> the coupling of the two indole rings of chromopyrrolic acid by StaP to form indolocarbazole in the biosynthesis of staurosporine,<sup>36</sup> and the dimerization of coniferyl alcohol monomers in the biosynthesis of lignin.<sup>37</sup> Incidentally, both salutaridine synthase and StaP are CYP-type oxygenases as well.<sup>35, 36</sup> Moreover, this proposed mechanism is in agreement with the [1,1- $^{18}\text{O}$ ]-acetate labeling study since all oxygen atoms are retained during the transformation of **11** to **14**.<sup>34</sup>

Alternatively, the oxidation of **11** by GsfF can go through an arene oxide intermediate (**11b**), which will then be subjected to nucleophilic attack by the hydroxyl of the phloroglucinol ring to form **11c**. The hemiacetal intermediate then undergoes dehydration to afford **14**. During the dehydration of the hemiacetal intermediate, the oxygen atom that originated from molecular oxygen is removed. Thus, this mechanism agrees as well with the labeling studies.<sup>34</sup> An analogous mechanism was proposed, along with a di-radical mechanism, in the ring coupling reaction by the CYP OxyB in the biosynthesis of the vancomycin family of antibiotics.<sup>38, 39</sup>

### GsfE performs stereospecific reduction of enol **18** to afford the final product **1**

Having functionally characterized the PKS GsfA, the MTs GsfB-D, the chlorinase GsfI and the P450 GsfF, the only uncharacterized biosynthetic step in the pathway is reduction of the cyclohexadienone ring in **18** or dechloro-dehydrogriseofulvin (**19**) to afford **1** or **2**, respectively. Two of the remaining uncharacterized genes in the cluster, *gsfE* and *gsfK*; are



for proteins that contain a conserved binding site for a nicotinamide cofactor and one of these may be capable of performing the final enoylreduction. Thus, single gene deletion mutants of *gsfE* and *gsfK* were constructed followed by metabolite analysis. All of the *gsfK* mutants isolated retained the ability to produce **1** and **2**. On the other hand, knockout of *gsfE* led to the production of **18** and **19** (Figure 4, iv), both of which were structurally verified by extensive NMR characterization (Supporting Information). Interestingly, while initial bioinformatic analysis of GsfE suggested that it is related to nucleoside-sugar epimerases based on sequence alignment, further analysis of the GsfE protein sequence via structural homology prediction revealed that it shares an overall folding, as well as conserved catalytic lysine and tyrosine as the progesterone-5 $\beta$ -reductase (POR) from the cardenolide biosynthetic pathway in *Digitalis lanata*.<sup>40</sup> POR catalyzes the stereospecific reduction of progesterone to form 5 $\beta$ -pregnane-3,20-dione, a reaction that is analogous to the reduction of the cyclohexadienone ring of **18** to form **1**. To verify the genetic and bioinformatic results, we reconstituted the reaction *in vitro* using His-tag fused-GsfE expressed and purified from *E. coli* BL21 (DE3), and **18** or **19** as substrates. NADPH was added as the reducing cofactor of GsfE. As shown in Figure 6A and Figure S5, GsfE fully converted **18** or **19** to **1** or **2**, respectively, thereby confirming its role as the last enzyme in the pathway. Moreover, this confirms GsfE performs a 1,4- (Michael-type) hydride addition instead a 1,2-addition performed by nucleoside sugar epimerases (Figure 6B).

### Total *in vitro* biosynthesis of **1** and **2**

Upon identifying all enzymatic components of the biosynthetic pathway, we attempted *in vitro* synthesis of **1** and **2** using purified Gsf enzymes (see Methods). Incubation of GsfA-F with malonyl-CoA, SAM and NADPH in PBS resulted in the expected production of **2** as a major product, along with **5**, **10** and **13**. Addition of GsfD-F after three-hour preincubation of GsfA-C with malonyl-CoA and SAM led to the production of **2** and **10** only. Finally, addition of the chlorinase GsfI and SsuE together with GsfA-F led to the production of the desired product **1** as a major product along with **2**, **10**, **11** and griseophenone A (**20**) (Figure 7, iii). The final yield of **1** with respect to malonyl-CoA was ~1%. The presence of **10** and **11** in all assays indicate the microsomal GsfF-catalyzed oxidative coupling is the rate limiting step in the multi-enzyme reactions.

Based on the results from the genetic and enzymatic data, we can establish the individual steps in the biosynthetic pathway for **1** (Scheme 3). The biosynthesis is initiated by the formation of the heptaketide by GsfA using one acetyl-CoA starter unit and six malonyl-CoA extender units. Thereafter, the product template (PT) domain of GsfA catalyzes the unprecedented C8-C13 aldol-type cyclization followed by C1-C6 Claisen-type cyclization to form **5a**, wherein dehydration of **5a** can readily take place in the absence of downstream steps to form the xanthone shunt product **5**. Meanwhile, on pathway processing of **5a** continues through the methylation at 3-OH and 9-OH by GsfB and GsfC, respectively, to form **10**. Although feeding studies by Harris *et al.* suggest that 3-OH methylation has priority over 9-OH methylation,<sup>16</sup> results from the knockout of *gsfB* and *gsfC* indicate that either can perform the first methylation reaction on the GsfA product **5a**. Following the two methylation steps, **10** undergoes chlorination by the flavin-dependent halogenase GsfI to form **11**. Following chlorination, **11** undergoes phenolic ring coupling by the cytochrome

P450 GsfF to form the grisan compound **14**. Subsequently, **14** is subjected to two additional tailoring steps: methylation at 5-OH and reduction of the cyclohexadienone to afford **1**. Based on the presence of **14** in the *gsfD* mutant, indicating the inefficient reduction by GsfE of the 5-OH-desmethyl substrates, it can be proposed that methylation by GsfD to yield **18** takes place before GsfE-catalyzed enoylreduction, which is in agreement with previous feeding studies on the biosynthesis of **1**.<sup>14-16, 34</sup> The chlorination step by GsfI is apparently incomplete in *P. aethiopicum* and *in vitro* (Figure 7). Enzymes downstream of GsfI, including GsfF, GsfD and GsfE, can all act on the respective dechlorinated substrates to yield the final product **2**. In conclusion, we performed comprehensive single-gene deletion of the *gsf* genes and functional characterization of the corresponding enzymes to elucidate the biosynthetic pathway of **1**. Several grisan analogues of **1** were isolated from the different gene deletion mutants (Scheme 1), hinting at the overall flexibility of the pathway and its potential for biosynthetic engineering. Moreover, this study has uncovered the novel and interesting reactions within this pathway, such as the unorthodox C1-C6 and C8-C13 cyclization of **5a** by GsfA, and P450-mediated ring coupling reaction of the orcinol and phloroglucinol rings of **11** to form **14**. These two reactions warrant further mechanistic investigations that may possibly lead to a better understanding of the biosynthesis of natural products with similar features.

## MATERIALS AND METHODS

### *In vitro* assay of GsfA

For the *in vitro* synthesis of **5**, 10  $\mu$ M GsfA was incubated with 2 mM malonyl-CoA and 15  $\mu$ M tailoring enzyme (Hpm TE, GsfB, GsfC or GsfD) in 100 mM phosphate buffered saline pH 7.4 in a 100  $\mu$ L reaction. The reaction was incubated overnight and extracted twice with ethyl acetate. For the reactions using malonyl-CoA generated *in situ* by MatB, the assay was done essentially the same as above except malonyl-CoA was substituted with 20  $\mu$ M MatB, 5mM CoA, 100 mM malonate, 5 mM MgCl<sub>2</sub>, 5mM DTT and 20 mM ATP. The organic phase was dried and dissolved in 20  $\mu$ L methanol and subjected to LCMS analysis as described in Supplemental Information.

### Chemical analysis and compound isolation from *P. aethiopicum* gene deletion mutants

For small-scale secondary metabolic profile analysis, the *P.aethiopicum* wild-type and transformants were grown in 10-20 mL YMEG liquid medium for 7 days at 28 °C without shaking. The cultures were extracted with equal volume of ethyl acetate with 1% acetic acid, evaporated to dryness and redissolved in methanol for LCMS analysis in the same manner as the *in vitro* characterization of GsfA (.). For preparative scale compound isolation, gene deletion strain of *P.aethiopicum* was grown in 3 L YMEG in the same manner as the small-scale cultures. The culture was extracted twice with equal volume of ethyl acetate and was evaporated to dryness and subjected to Sephadex and HPLC purification and NMR characterization in the same manner as **5**.

### *In vitro* assay of GsfI

The assay for the chlorinase was done essentially the same as described in Zhou *et al.*<sup>41</sup> Briefly, 50  $\mu$ M of GsfI was incubated with 200  $\mu$ M Griseophenone C (**10**) in 100 mM



sodium phosphate buffer (pH 7.4) and 50 mM NaCl. In order to regenerate the reduced flavin in GsfI, the flavin reductase SsuE (15  $\mu$ M), FAD (5  $\mu$ M) and NADPH (2 mM) were added to the reaction mix. After overnight incubation, the reaction mix was extracted twice with equal volume ethyl acetate, dried *in vacuo* and subjected to LCMS analysis as described above for **5**.

### ***In vitro* assay of GsfE**

For *in vitro* synthesis of **1** from **18**, 10  $\mu$ M of GsfE was incubated with 100  $\mu$ M and 1 mM NADPH in 100 mM Tris-HCl (pH 7.5) buffer and 100  $\mu$ L reaction volume. After 5 hour incubation in room temperature, the reaction mix was extracted twice with equal volume of ethyl acetate, dried *in vacuo* and analyzed by LCMS in the same manner as **5**.

### **Total *in vitro* biosynthesis of 1 and 2**

For the total *in vitro* synthesis of **2**, 4  $\mu$ M of GsfA, 2  $\mu$ M each of the methyltransferases (GsfB, GsfC and GsfD), 2  $\mu$ L of microsomal protein containing GsfF and AtCPR and 2  $\mu$ M of GsfE were incubated with 2 mM of malonyl-CoA, 100  $\mu$ M of *S*-adenosyl methionine and 2 mM of NADPH in 100  $\mu$ L reaction mix buffered with 100 mM sodium phosphate (pH 7.4) and 50 mM NaCl. After overnight incubation, the reaction mix was extracted twice with equal volume ethyl acetate, dried and subjected to the same LCMS analysis as **5** (*vide supra*). The total *in vitro* biosynthesis of **1** was done in the same manner as **2**, except GsfA-C were incubated with 10  $\mu$ M of GsfI and 2  $\mu$ M SsuE for 3 hours prior to addition of GsfF, GsfE and GsfD. The total yield of **1** was measured by comparing the area under the chromatogram peak of **1** against a standard curve of known amount of **1** injected and analyzed by LCMS.

## **Supplementary Material**

Refer to Web version on PubMed Central for supplementary material.

## **ACKNOWLEDGMENT**

This work is supported by NIH grants 1R01GM085128 and 1DP1GM106401 to Y.T.; and NRSA GM-0846 and the UCLA Graduate Division to R.A.C. NMR instrumentation was supported by the NSF equipment grant CHE-1048804. We thank D-K Ro for providing the pESC-*Leu*-AtCPR plasmid for the P450 reconstitution. We express our sincere gratitude to J.C. Vederas for helpful discussion on the biosynthetic routes.

## **ABBREVIATIONS**

<b>PKS</b>	polyketide synthase
<b>TE</b>	thioesterase domain
<b>CYP</b>	cytochrome P450
<b>SAM</b>	<i>S</i> -adenosyl methionine
<b>SAH</b>	<i>S</i> -adenosyl homocysteine
<b>NADPH</b>	nicotinamide adenine dinucleotide phosphate (reduced)

## REFERENCES

1. Frisvad JC, Samson RA. Polyphasic taxonomy of *Penicillium* subgenus *Penicillium*. A guide to identification of food and air-borne terverticillate *Penicillia* and their mycotoxins. *Studies in Mycology*. 2004; 49:1–174.
2. Gentles JC. Experimental ringworm in guinea pigs: oral treatment with griseofulvin. *Nature*. 1958; 182:476–477. [PubMed: 13577889]
3. Pillsbury DM. Griseofulvin therapy in dermatophytic infections. *Trans Am Clin Climatol Assoc*. 1960; 71:52–57. [PubMed: 14433006]
4. Gull K, Trinci APJ. Griseofulvin inhibits fungal mitosis. *Nature*. 1973; 244:292–294. [PubMed: 4583105]
5. Finkelstein E, Amichai B, Grunwald MH. Griseofulvin and its uses. *Int J Antimicrob Agents*. 1996; 6:189–194. [PubMed: 18611708]
6. Panda D, Rathinasamy K, Santra MK, Wilson L. Kinetic suppression of microtubule dynamic instability by griseofulvin: Implications for its possible use in the treatment of cancer. *Proc Natl Acad Sci USA*. 2005; 102:9878–9883. [PubMed: 15985553]
7. Rebacz B, Larsen TO, Clausen MH, Rønneest MH, Löffler H, Ho AD, Krämer A. Identification of griseofulvin as an inhibitor of centrosomal clustering in a phenotype-based screen. *Cancer Res*. 2007; 67:6342–6350. [PubMed: 17616693]
8. Hutchinson CR. The use of isotopic hydrogen and nuclear magnetic resonance spectroscopic techniques for the analysis of biosynthetic pathways. *J Nat Prod*. 1982; 45:27–37.
9. Birch AJ, Massy-Westropp RA, Rickards RW, Smith H. 66. Studies in relation to biosynthesis. Part XIII. Griseofulvin. *J Chem Soc*. 1958; 0:360–365.
10. Birch A, Donovan F. Studies in relation to biosynthesis. I. Some possible routes to derivatives of orcinol and phloroglucinol. *Aus J Chem*. 1953; 6:360–368.
11. Staunton J, Weissman KJ. Polyketide biosynthesis: a millennium review. *Nat Prod Rep*. 2001; 18:380–416. [PubMed: 11548049]
12. Simpson TJ, Holker JSE. <sup>13</sup>C-NMR studies on griseofulvin biosynthesis and acetate metabolism in *Penicillium patulum*. *Phytochemistry*. 1977; 16:229–233.
13. Barton, DHR.; Cohen, T. In *Festschrift Prof. Dr. Arthur Stoll*. Birkhauser; Basel: 1957.
14. Rhodes A, Boothroyd B, Mc GP, Somerfield GA. Biosynthesis of griseofulvin: the methylated benzophenone intermediates. *Biochem J*. 1961; 81:28–37. [PubMed: 14491779]
15. Rhodes A, Somerfield GA, McGonagle MP. Biosynthesis of griseofulvin. Observations on the incorporation of [<sup>14</sup>C]Griseophenone C and [<sup>36</sup>Cl]Griseophenones B and A. *Biochem J*. 1963; 88:349–357. [PubMed: 14063874]
16. Harris CM, Roberson JS, Harris TM. Biosynthesis of griseofulvin. *J Am Chem Soc*. 1976; 98:5380–5386. [PubMed: 956563]
17. Chooi Y-H, Cacho R, Tang Y. Identification of the viridicatumtoxin and griseofulvin gene clusters from *Penicillium aethiopicum*. *Chem Biol*. 2010; 17:483–494. [PubMed: 20534346]
18. Gao X, Chooi Y-H, Ames BD, Wang P, Walsh CT, Tang Y. Fungal indole alkaloid biosynthesis: genetic and biochemical investigation of the tryptoquialanine pathway in *Penicillium aethiopicum*. *J Am Chem Soc*. 2011; 133:2729–2741. [PubMed: 21299212]
19. Ma SM, Li JW-H, Choi JW, Zhou H, Lee KKM, Moorthis VA, Xie X, Kealey JT, Da Silva NA, Vederas JC, Tang Y. Complete reconstitution of a highly reducing iterative polyketide synthase. *Science*. 2009; 326:589–592. [PubMed: 19900898]
20. Zhou H, Qiao K, Gao Z, Meehan MJ, Li JWH, Zhao X, Dorrestein PC, Vederas JC, Tang Y. Enzymatic synthesis of resorcyclic acid lactones by cooperation of fungal iterative polyketide synthases involved in hypothemycin biosynthesis. *J Am Chem Soc*. 2010; 132:4530–4531. [PubMed: 20222707]
21. Crawford JM, Dancy BCR, Hill EA, Udway DW, Townsend CA. Identification of a starter unit acyl-carrier protein transacylase domain in an iterative type I polyketide synthase. *Proc Natl Acad Sci USA*. 2006; 103:16728–16733. [PubMed: 17071746]

22. Crawford JM, Korman TP, Labonte JW, Vagstad AL, Hill EA, Kamari-Bidkorpheh O, Tsai S-C, Townsend CA. Structural basis for biosynthetic programming of fungal aromatic polyketide cyclization. *Nature*. 2009; 461:1139–1143. [PubMed: 19847268]
23. Crawford JM, Thomas PM, Scheerer JR, Vagstad AL, Kelleher NL, Townsend CA. Deconstruction of iterative multidomain polyketide synthase function. *Science*. 2008; 320:243–246. [PubMed: 18403714]
24. Korman TP, Crawford JM, Labonte JW, Newman AG, Wong J, Townsend CA, Tsai S-C. Structure and function of an iterative polyketide synthase thioesterase domain catalyzing Claisen cyclization in aflatoxin biosynthesis. *Proc Natl Acad Sci USA*. 2010; 107:6246–6251. [PubMed: 20332208]
25. Fujii I, Watanabe A, Sankawa U, Ebizuka Y. Identification of Claisen cyclase domain in fungal polyketide synthase WA, a naphthopyrone synthase of *Aspergillus nidulans*. *Chem Biol*. 2001; 8:189–197. [PubMed: 11251292]
26. Cox RJ. Polyketides, proteins and genes in fungi: programmed nano-machines begin to reveal their secrets. *Org Biomol Chem*. 2007; 5:2010–2026. [PubMed: 17581644]
27. Chooi Y-H, Tang Y. Navigating the fungal polyketide chemical space: from genes to molecules. *J Org Chem*. 2012; 77:9933–9953. [PubMed: 22938194]
28. Townsend CA, Crawford JM. New insights into the formation of fungal aromatic polyketides. *Nat Rev Micro*. 2012; 8:879–889.
29. Li Y, Xu W, Tang Y. Classification, prediction, and verification of the regioselectivity of fungal polyketide synthase product template domains. *J Biol Chem*. 2010; 285:22764–22773. [PubMed: 20479000]
30. Li Y, Chooi Y-H, Sheng Y, Valentine JS, Tang Y. Comparative characterization of fungal anthracenone and naphthacenedione biosynthetic pathways reveals an  $\alpha$ -hydroxylation-dependent Claisen-like cyclization catalyzed by a dimanganese thioesterase. *J Am Chem Soc*. 2011; 133:15773–15785. [PubMed: 21866960]
31. Peres V, Nagem TJ. Trioxxygenated naturally occurring xanthenes. *Phytochemistry*. 1997; 44:191–214.
32. Huang, K.-x.; Fujii, I.; Ebizuka, Y.; Gomi, K.; Sankawa, U. Molecular cloning and heterologous expression of the gene encoding dihydrogeodin oxidase, a multicopper blue enzyme from *Aspergillus terreus*. *J Biol Chem*. 1995; 270:21495–21502. [PubMed: 7665560]
33. Partow S, Siewers V, Bjørn S, Nielsen J, Maury J. Characterization of different promoters for designing a new expression vector in *Saccharomyces cerevisiae*. *Yeast*. 2010; 27:955–964. [PubMed: 20625983]
34. Lane MP, Nakashima TT, Vederas JC. Biosynthetic source of oxygens in griseofulvin. Spin-echo resolution of oxygen-18 isotope shifts in carbon-13 NMR spectroscopy. *J Am Chem Soc*. 1982; 104:913–915.
35. Gesell A, Rolf M, Ziegler J, Díaz Chávez ML, Huang F-C, Kutchan TM. CYP719B1 Is salutaridine synthase, the C-C phenol-coupling enzyme of morphine biosynthesis in opium poppy. *J Biol Chem*. 2009; 284:24432–24442. [PubMed: 19567876]
36. Makino M, Sugimoto H, Shiro Y, Asamizu S, Onaka H, Nagano S. Crystal structures and catalytic mechanism of cytochrome P450 StaP that produces the indolocarbazole skeleton. *Proc Natl Acad Sci USA*. 2007; 104:11591–11596. [PubMed: 17606921]
37. Vanholme R, Demedts B, Morreel K, Ralph J, Boerjan W. Lignin biosynthesis and structure. *Plant Physiol*. 2010; 153:895–905. [PubMed: 20472751]
38. Zerbe K, Woihte K, Li DB, Vitali F, Bigler L, Robinson JA. An oxidative phenol coupling reaction catalyzed by OxyB, a cytochrome P450 from the vancomycin-producing microorganism. *Angew Chem Int Ed*. 2004; 43:6709–6713.
39. Holding AN, Spencer JB. Investigation into the mechanism of phenolic couplings during the biosynthesis of glycopeptide antibiotics. *ChemBioChem*. 2008; 9:2209–2214. [PubMed: 18677741]
40. Thorn A, Egerer-Sieber C, Jäger CM, Herl V, Müller-Uri F, Kreis W, Muller YA. The crystal structure of progesterone 5 $\beta$ -reductase from *Digitalis lanata* defines a novel class of short chain dehydrogenases/reductases. *J Biol Chem*. 2008; 283:17260–17269. [PubMed: 18032383]

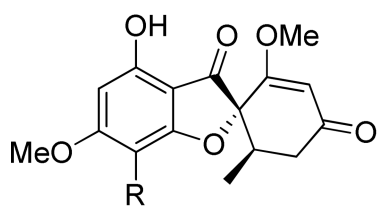
41. Zhou H, Qiao K, Gao Z, Vederas J, Tang Y. Insights into radicicol biosynthesis via heterologous synthesis of intermediates and analogs. *J Biol Chem.* 2010; 285:41412–41421. [PubMed: 20961859]

Author Manuscript

Author Manuscript

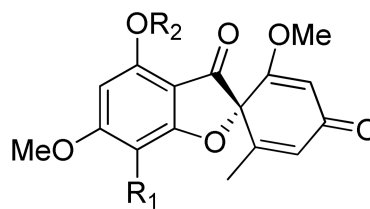
Author Manuscript

Author Manuscript



R= H, Desmethyl-dechlorogriseofulvin (**13**)

R= Cl, Desmethylgriseofulvin (**15**)



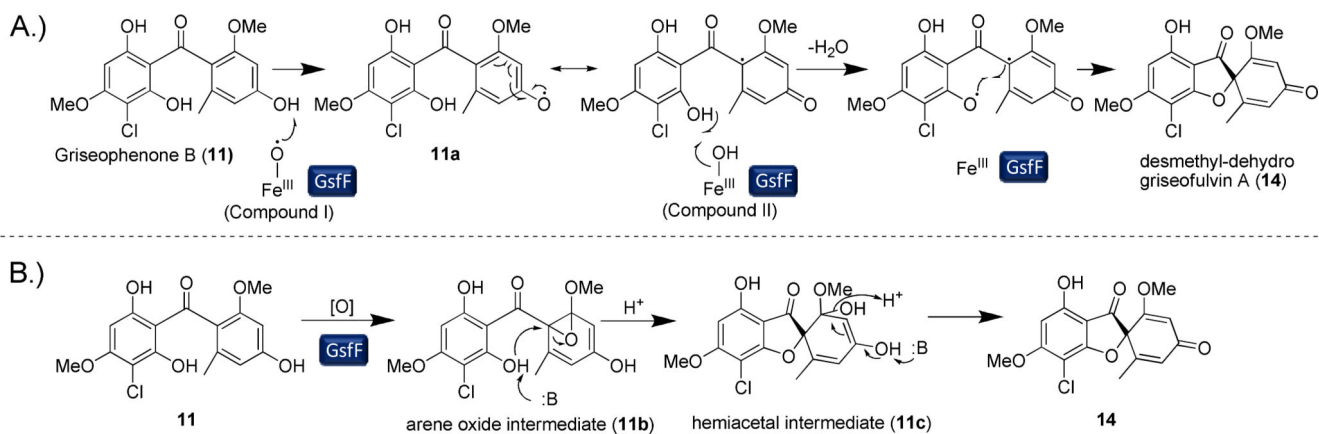
R<sub>1</sub>= Cl, R<sub>2</sub> = H, Desmethyl-dehydrogriseofulvin A (**14**)

R<sub>1</sub>= Cl, R<sub>2</sub>=CH<sub>3</sub>, Dehydrogriseofulvin (**18**)

R<sub>1</sub>= H, R<sub>2</sub>=CH<sub>3</sub>, Dechloro-dehydrogriseofulvin (**19**)

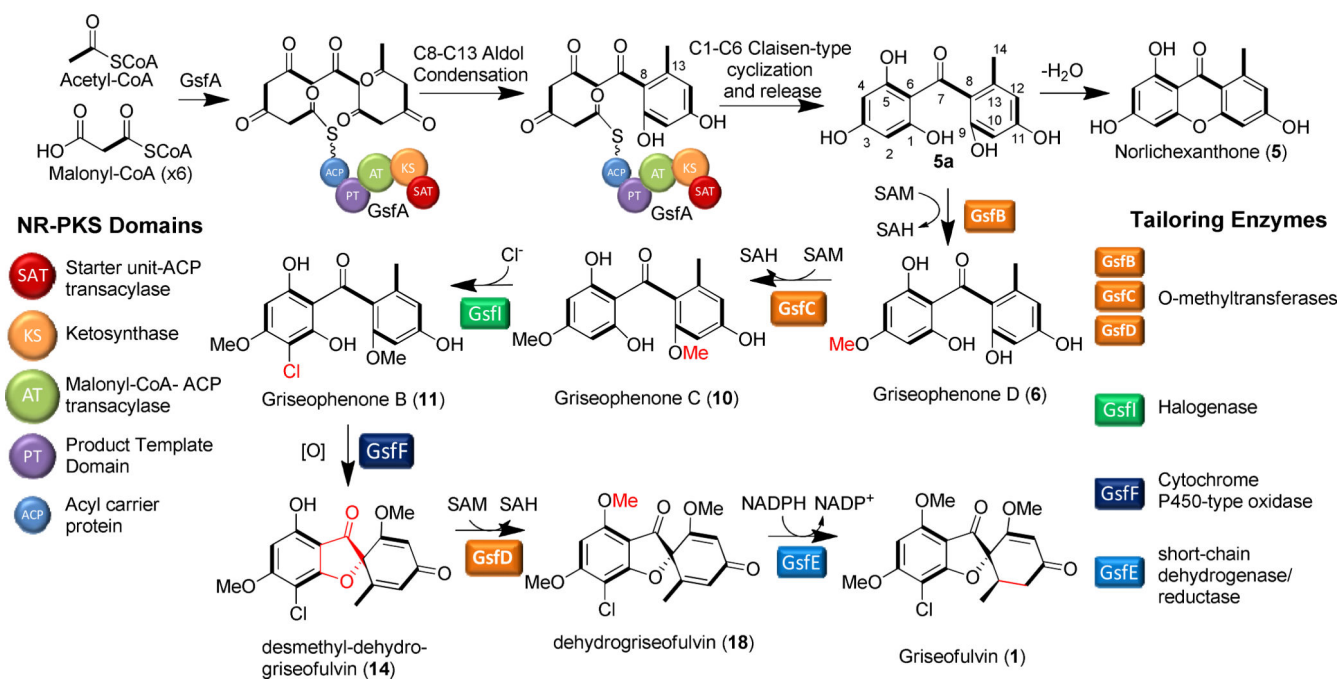
**Scheme 1.**

Shunt products and intermediates that contain the grisan scaffold.

**Scheme 2.**

Putative mechanisms of the orcinol and phloroglucinol ring coupling by GsfF. A.) Di-radical ring coupling mechanism of GsfF. B.) Alternative mechanism for the ring coupling involving an arene oxide intermediate.





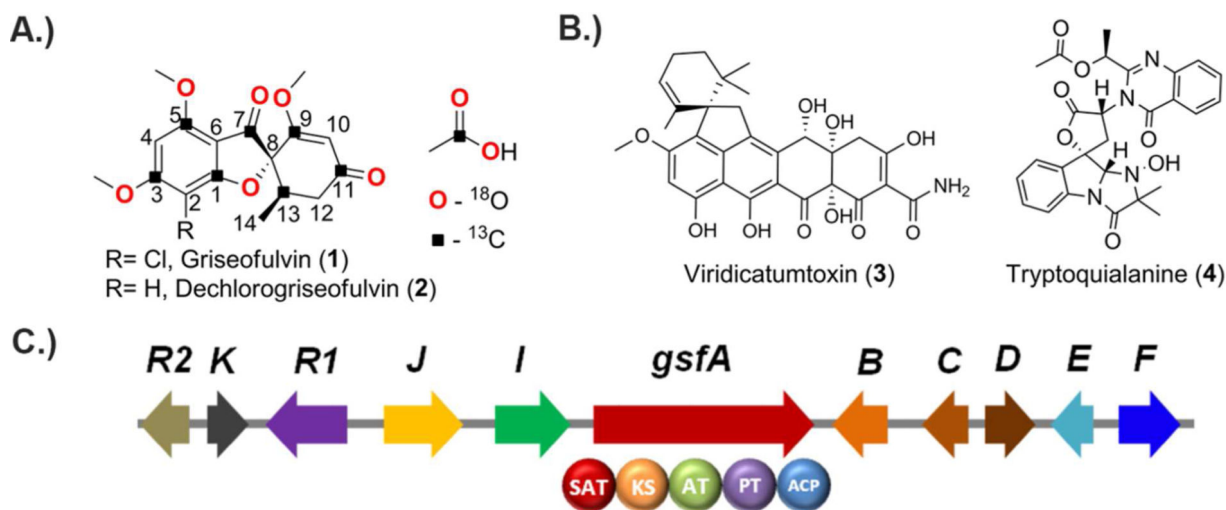


**Figure 1.** Griseofulvin (**1**) and other secondary metabolites produced by *Penicillium aethiopicum*. **A.)** The structure of **1** and dechlorogriseofulvin (**2**) shown together with the acetate origin of carbon and oxygen atoms. **B.)** Viridicatumtoxin (**3**) and tryptoquialanine (**4**) are the other chemotaxonomic marker in *P. aethiopicum*; and **C.)** Arrangement of genes in the biosynthetic gene cluster of **1** in *P. aethiopicum*.

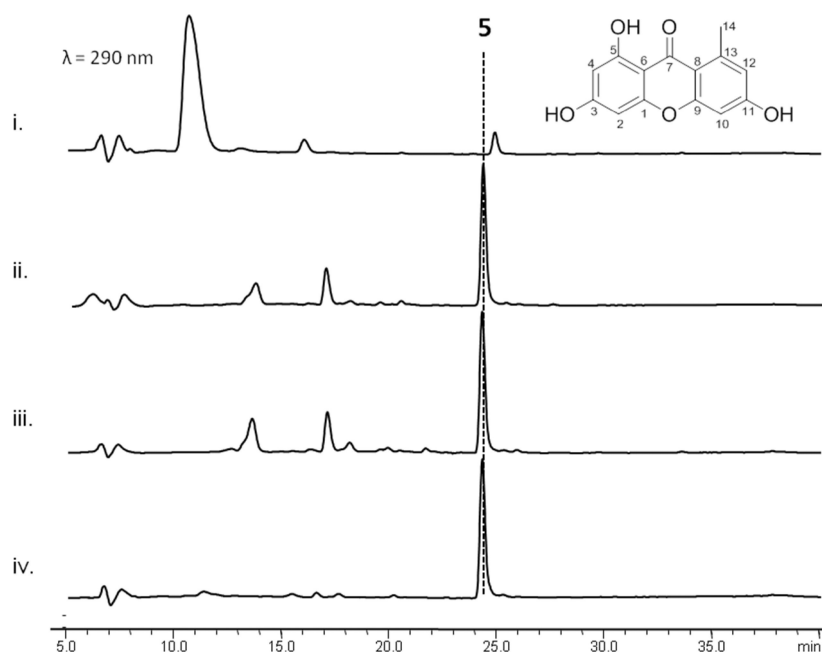


**Figure 2.** GsfA catalyzes formation of **5** from malonyl-CoA as confirmed by HPLC analysis. i.) No GsfA control ii.) GsfA and the excised TE domain of Hpm3 incubated with *in situ* generated malonyl-CoA. iii.) GsfA incubated with *in situ* generated malonyl-CoA using MatB, malonate, CoA and ATP. iv.) GsfA incubated with malonyl-CoA only.

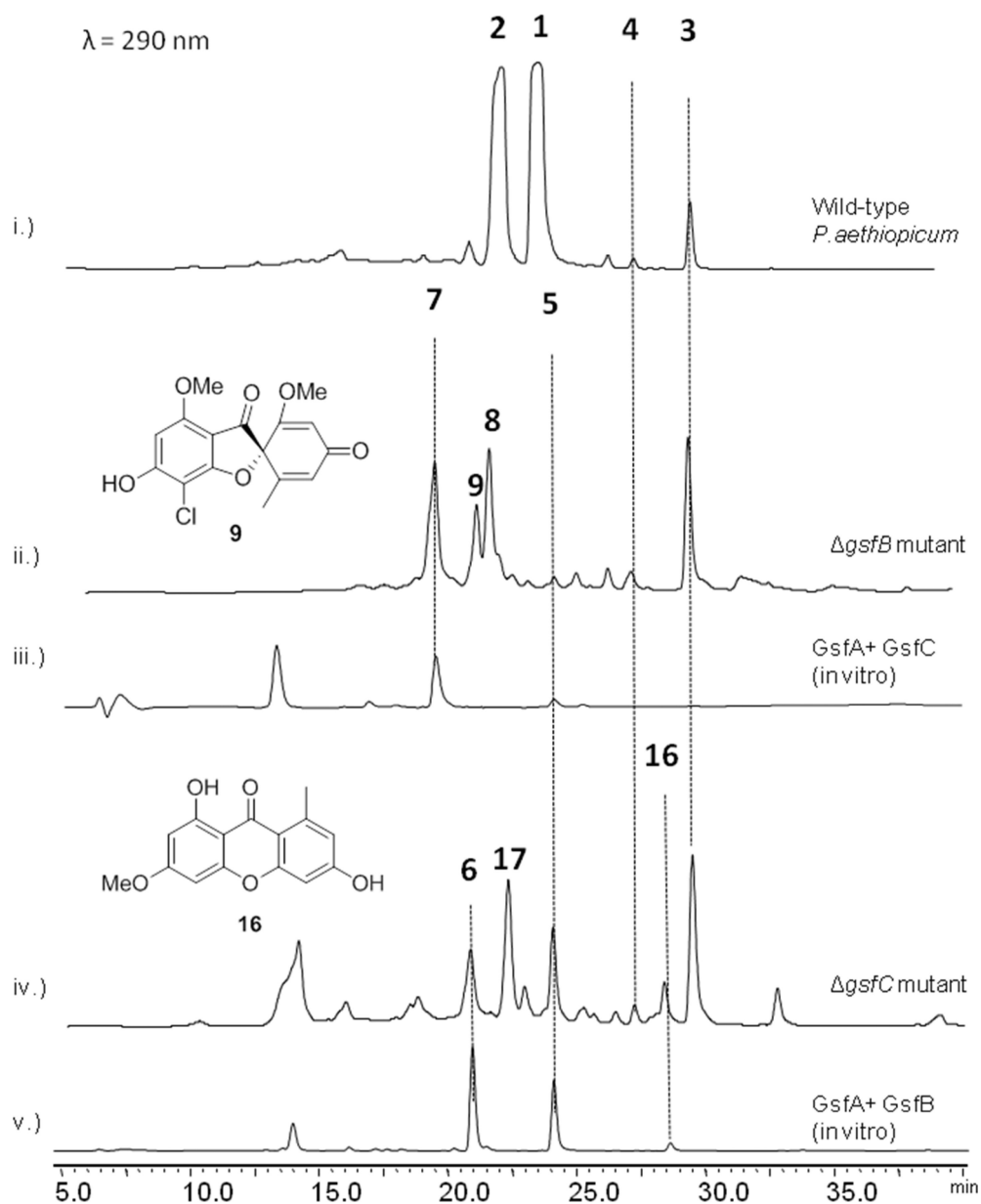


**Figure 3.** The *O*-methyltransferases GsfB and GsfC tailor the nascent GsfA product. i.) Secondary metabolic profile of *Penicillium aethiopicum* showing the production of 1-4. ii.) Deletion of *gsfB* led to the production of 5, 7, 8, and 9. iii.) Coupled *in vitro* assay of GsfA and GsfC led to the production of 7 thereby confirming 9-OH regioselectivity of GsfC iv.) Deletion of *gsfC* led to the production of 5, 6, 16 and 17. v.) Coupled *in vitro* assay of GsfA and GsfB led to the production of 5, 6 and 16 thereby confirming the 3-OH regioselectivity of GsfB.

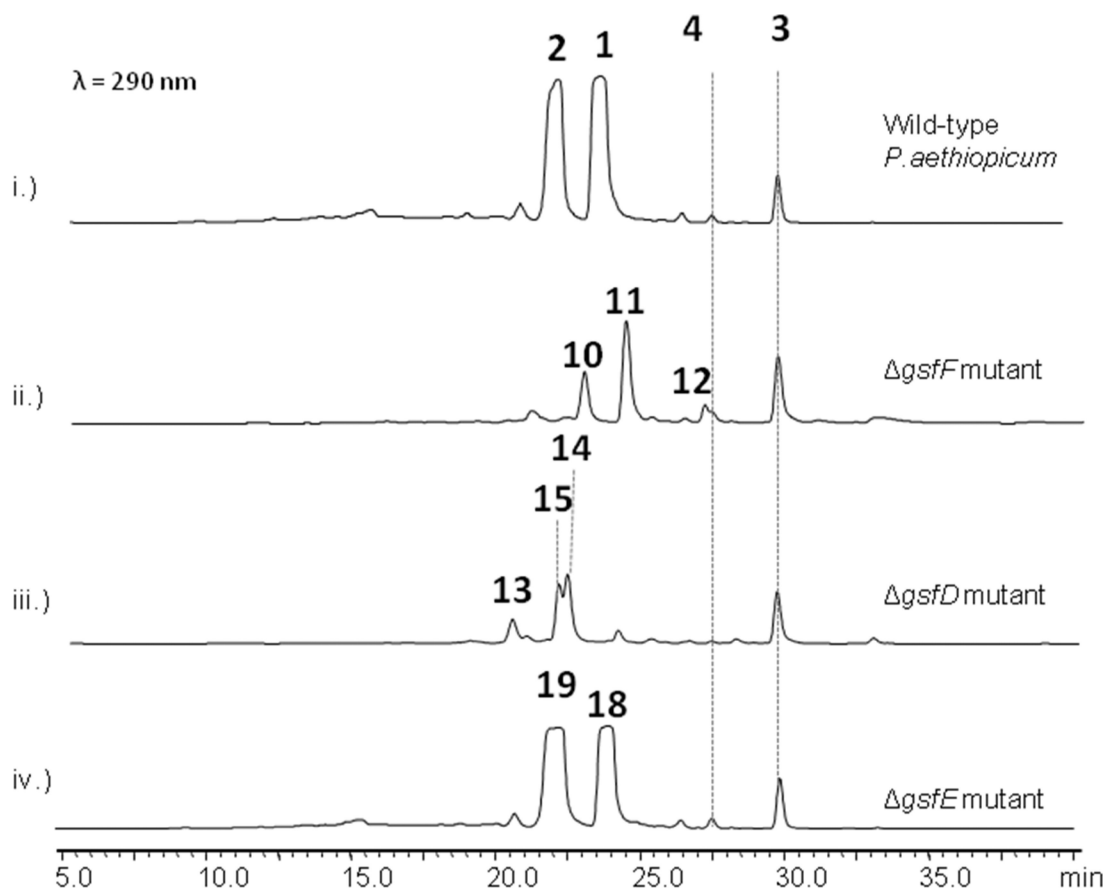


**Figure 4.**

Tailoring reactions in biosynthesis of **1**. i.) Wild-type *P.aethiopicum* showing the production of **1-4**. ii.) Knockout of cytochrome P450 gene *gsfF* led to the production of the dimethylated phenones **10**, **11** & **12** containing different degrees of chlorination. iii.) Knockout of the *O*-methyltransferase *gsfD* led to the production of **13**, **14** and **15**. iv.) Knockout of the short-chain dehydrogenase /reductase gene *gsfE* led to the production of **18**, and **19**.

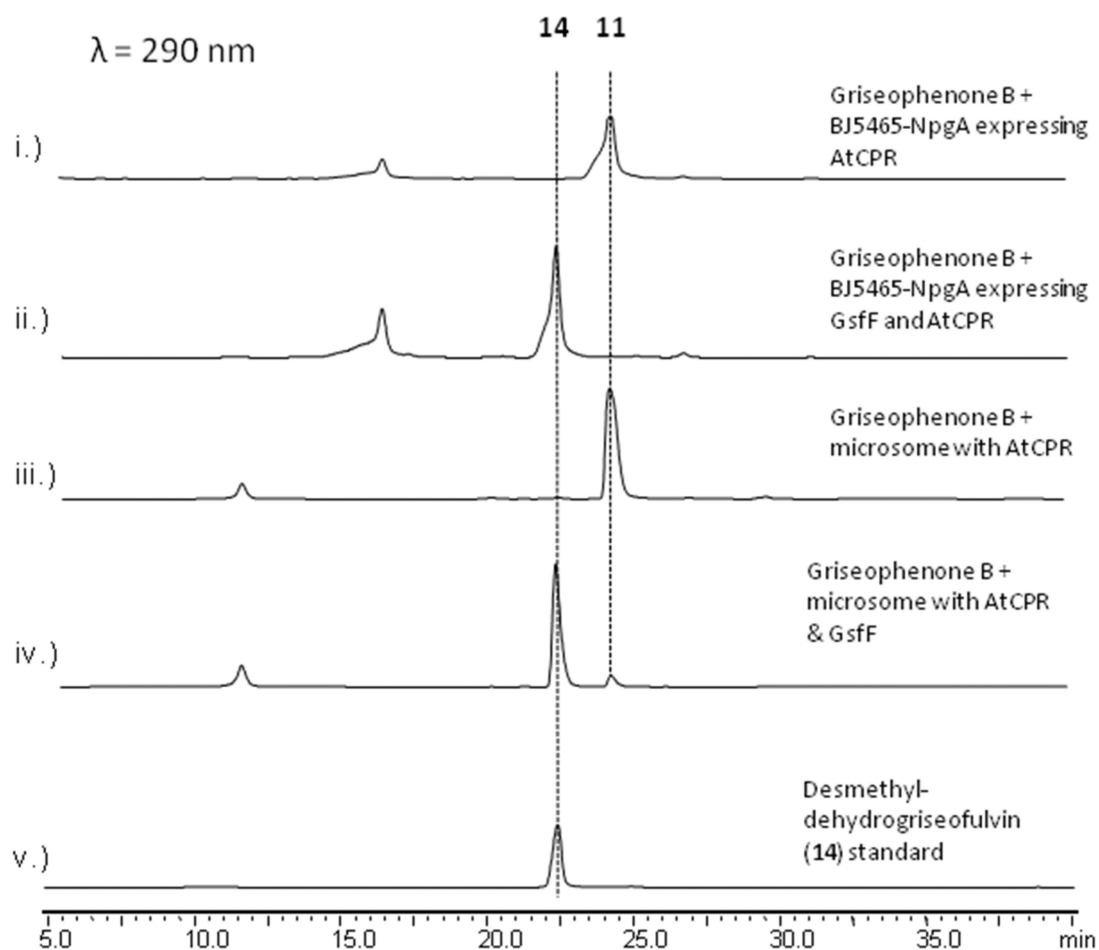


**Figure 5.**

The cytochrome P450 GsfF catalyzes the coupling of orcinol and phloroglucinol rings in griseophenone B (**11**) to form desmethyl-dehydrogriseofulvin A (**14**). i.) BJ5464-NpgA expressing CPR only did not convert **11** to **14**. ii.) BJ5464-NpgA expressing both CPR and GsfF completely converted **11** to **14** after 24 hours. iii.) Yeast microsomes containing CPR do not convert **11** in vitro. iv.) Yeast microsomes containing both CPR and GsfF converted **11** to **14** in the presence of NADPH. v.) Standard of **14** purified from *gsfD* deletion strain.



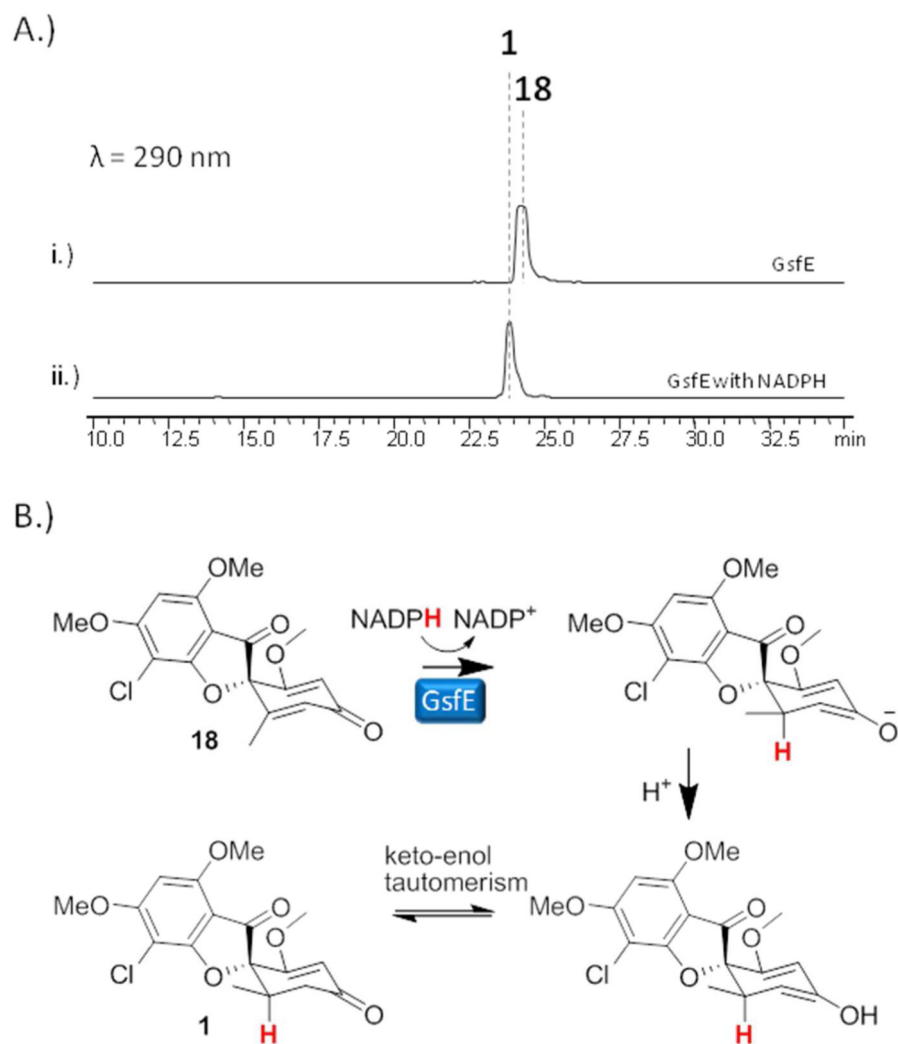


**Figure 6.** Verifying the activity of GsfE. A.) Incubation of **18** with 10 M GsfE and 1 mM NADPH led to the production of **1**. B.) Putative mechanism of GsfE showing the stereospecific 1,4- (Michael) addition of the hydride from NADPH to **18**, followed by protonation of the resulting cyclohexadienolate to form **1**.

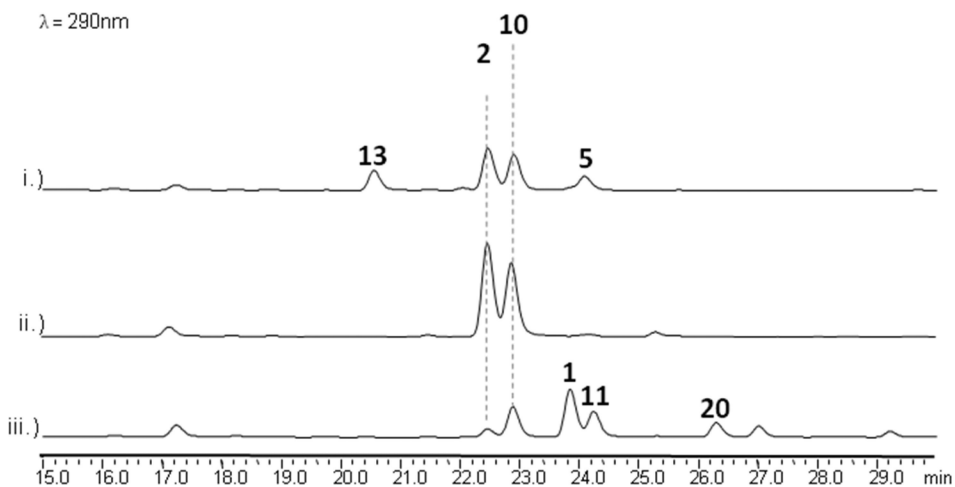


**Figure 7.**

*In vitro* total biosynthesis of **1** and **2**. i.) GsfA-F, SAM and malonyl-CoA added in one step.

ii.) GsfA-C, SAM and malonyl-CoA incubated together for 3 hours prior to addition of

NADPH, GsfF, GsfD and GsfE. iii.) GsfA-C, GsfI, SsuE, SAM, malonyl-CoA and NADPH

incubated together for 3 hours prior to addition of GsfF, GsfD and GsfE.

**Table 1**

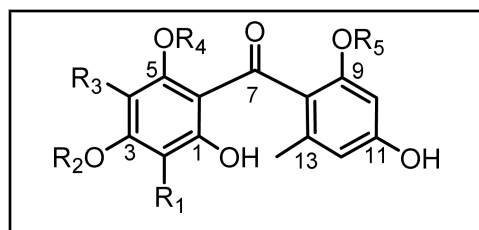
Putative functions of the genes in the **1** biosynthetic pathway and identified metabolites from single-gene knockout strains.\*

<b>Gene</b>	<b>Function</b>	<b>Identified metabolites from KO strains</b>
<i>gsfA</i>	NR-PKS (SAT-KS-AT-PT-ACP)	None *
<i>gsfB</i>	(3-OH) <i>O</i> -methyltransferase	<b>5, 7, 8, 9</b>
<i>gsfC</i>	(9-OH), <i>O</i> -methyltransferase	<b>6, 16, 17</b>
<i>gsfD</i>	(5-OH), <i>O</i> -methyltransferase	<b>13, 14, 15</b>
<i>gsfE</i>	short-chain dehydrogenase/reductase	<b>18, 19</b>
<i>gsfF</i>	cytochrome P450	<b>10, 11, 12</b>
<i>gsfI</i>	halogenase	<b>2</b> *
<i>gsfK</i>	ketoreductase	<b>1, 2</b>

\* Knockout of *gsfA* and *gsfI* was reported in a previous study by our group (ref 17).

**Table 2**

Griseophenones characterized in this study.



Compound	R <sub>1</sub>	R <sub>2</sub>	R <sub>3</sub>	R <sub>4</sub>	R <sub>5</sub>
<b>5a</b>	H	H	H	H	H
griseophenone D ( <b>6</b> )	H	Me	H	H	H
griseophenone E ( <b>7</b> )	H	H	H	H	Me
griseophenone F ( <b>8</b> )	Cl	H	H	H	Me
griseophenone C ( <b>10</b> )	H	Me	H	H	Me
griseophenone B ( <b>11</b> )	Cl	Me	H	H	Me
griseophenone G ( <b>12</b> )	Cl	Me	Cl	H	Me
griseophenone H ( <b>17</b> )	Cl	Me	H	H	H
griseophenone A ( <b>20</b> )	Cl	Me	H	Me	Me